Self-adhesive and Self-healing Hydrogel Dressings based on Quaternary Ammonium Chitosan and Host-guest Interacted Silk Fibroin

Wei Guo[a], Xinyue Gao[a], Xiaoyue Ding[a], Peng Ding[a], Yanting Han[a], Qingping Guo[a], Yixian Ma[a], Oseweuba Valentine Okoro[b], Yanfang Sun[c], Guohua Jiang[d,e], Mahta Mirzaei[f,g], Amin Shavandi[b], and Lei Nie[a,*]

[a] College of Life Sciences, Xinyang Normal University, Xinyang 464000, China.

[b] Université libre de Bruxelles (ULB), École polytechnique de Bruxelles, 3BIO-BioMatter, Avenue F.D. Roosevelt, 50 - CP 165/61, 1050 Brussels, Belgium.

[c] College of Life Sciences and Medicine, Zhejiang Sci-Tech University, Hangzhou 310018, China

[d] School of Materials Science and Engineering, Zhejiang Sci-Tech University, Hangzhou 310018, China

[e] International Scientific and Technological Cooperation Base of Intelligent Biomaterials and Functional Fibers, Zhejiang Sci-Tech University, Hangzhou 310018, China

[f] Centre for Food Chemistry and Technology, Ghent University Global Campus, Incheon, South Korea.

[g] Department of Food Technology, Safety and Health, Faculty of Bioscience Engineering, Ghent University, Coupure Links 653, geb. A, B-9000 Ghent, Belgium.

Corresponding author: Prof. Lei Nie

Tel: +86-13600621068. ORCID: 0000-0002-6175-5883

E-mail address: nieleifu@yahoo.com; nielei@xynu.edu.cn

Abstract

Skin is susceptible to varying degrees of injury from external forces, heat, disease, and chemical corrosion. Wound dressings using tissue engineering principles can accelerate skin tissue repair, relieve patient pain, and reduce the formation of scars. In this study, the self-adhesive and self-healing hydrogel dressings based on quaternary ammonium chitosan (QCS), β-cyclodextrin-modified silk fibroin (CD-SF), and adamantane-modified silk fibroin (AD-SF), that was designed. The formed hydrogels not only based on the host-guest interactions between CD-SF as host polymer and AD-SF as guest polymer, also the hydrogen-bonding assembly from QCS was combined. The successful synthesis of QCS, CD-SF, and AD-SF was established using Fourier Transform Infrared spectroscopy (FT-IR) and ^{1}H nuclear magnetic resonance (^{1}H NMR) spectroscopy. The obtained QCS/CD-SF/AD-SF (QCA) hydrogels displayed self-adhesive, self-healing, and mechanical properties. The hydrogels exhibited antibacterial performance, combating typical Gram-negative bacteria *Escherichia coli* (*E. coli*) and Gram-positive bacteria *Staphylococcus aureus* (*S. aureus*). Further, CCK-8 assay by incubating hydrogels with NIH-3T3 cells and optical microscope inspection of cell morphology indicates the excellent cytocompatibility of the hydrogels. The designed QCA hydrogel with antibacterial properties and biocompatibility have great potential as wound dressings for wound healing treatment.

Keywords

Hydrogels; chitosan; silk fibroin; wound dressing; antibacterial properties

1 Introduction

The skin plays a vital role in protecting against pathogenic microorganisms, water loss, and chemical and physical attacks [1, 2]. After skin injury, wound healing works through a series of coordinated molecular and cellular processes to repair damaged tissue [3]. Scientists worldwide seek an ideal wound dressing that speeds up impaired wound healing. The available options include films, foams, composites, sprays, nanoparticles and hydrogels, all designed wound dressings to act as barriers to promote wound repairs [4-6]. Hydrogels, particularly, have earned considerable attention owing to their three-dimensional (3D) network structure, providing a moist environment, potential antibacterial properties and biocompatibility[7-10]. Hydrogels are essential biomaterials with excellent biocompatibility, swelling, and mechanical properties similar to soft tissue extracellular matrix [11].

Among the diverse range of natural polymers, chitosan (CS) is a cationic polymer known for its antibacterial activity [12, 13]. The derivative of CS known as QCS, exhibits favorable solubility, which can be challenging when considering the use of CS as wound dressings for wound healing [14-17]. Creating a multi-functional hydrogel dressing with a single QCS, especially one with strong mechanical and self-healing properties, is challenging [18-21]. Incorporating other natural polymers alongside QCS is an approach to further enhance hydrogels' physicochemical properties. In addition, silk fibroin (SF) has been widely utilized in wound dressing because of its capability for oxygen transmission, strong mechanical properties, good biocompatibility, and degradability [22-25]. Furthermore, SF protein has been

reported to promote cell adhesion, foster re-epithelialization and hemostasis, reduce immune response, accelerate the process of wound repair, and promote wound healing [26-28]. Many studies have shown that the composite of SF and CS exhibits good antibacterial and mechanical properties as wound dressings [18, 19, 29]. However, the supramolecular hydrogel has not been reported based on chemically modified SF and CS composites as novel wound dressing.

Here, we report an innovative approach to fabricating self-adhesive and self-healing hydrogel through host-guest complexation. The host-guest effect refers to the phenomenon in which two molecules form a reversible, non-covalent self-assembly to create an inclusion complex [30, 31]. This connection arises from physical interaction that entails the incorporation of a guest molecule into the primary structure of host molecules to form a unique structural relationship [32, 33]. In our research, CD-SF serves as a host molecule, while AD-SF is a guest molecule. Additionally, we introduced QCS into the host-guest interacted hydrogel structure to further improve its physicochemical properties via hydrogen-bonding assembly, also possessing its antimicrobial properties. The developed hydrogels, QCA, were assessed for use as wound dressings. The characterizations of the developed QCA hydrogels were evaluated using techniques such as FT-IR and Scanning Electron Microscope (SEM) image analysis. The rheology analysis was determined to test the hydrogels' mechanical properties. Antibacterial and antioxidant activities and biocompatibility of developed hydrogel were also measured. Our experiments provide evidence and fundamental data for applying the QCA hydrogels as wound dressings. In this study,

the QCA hydrogels were successfully synthesized. The schematic representation of the synthesis of QCS, CD-SF, and AD-SF, as well as the fabrication of QCA hydrogels, are shown in **Scheme 1**.

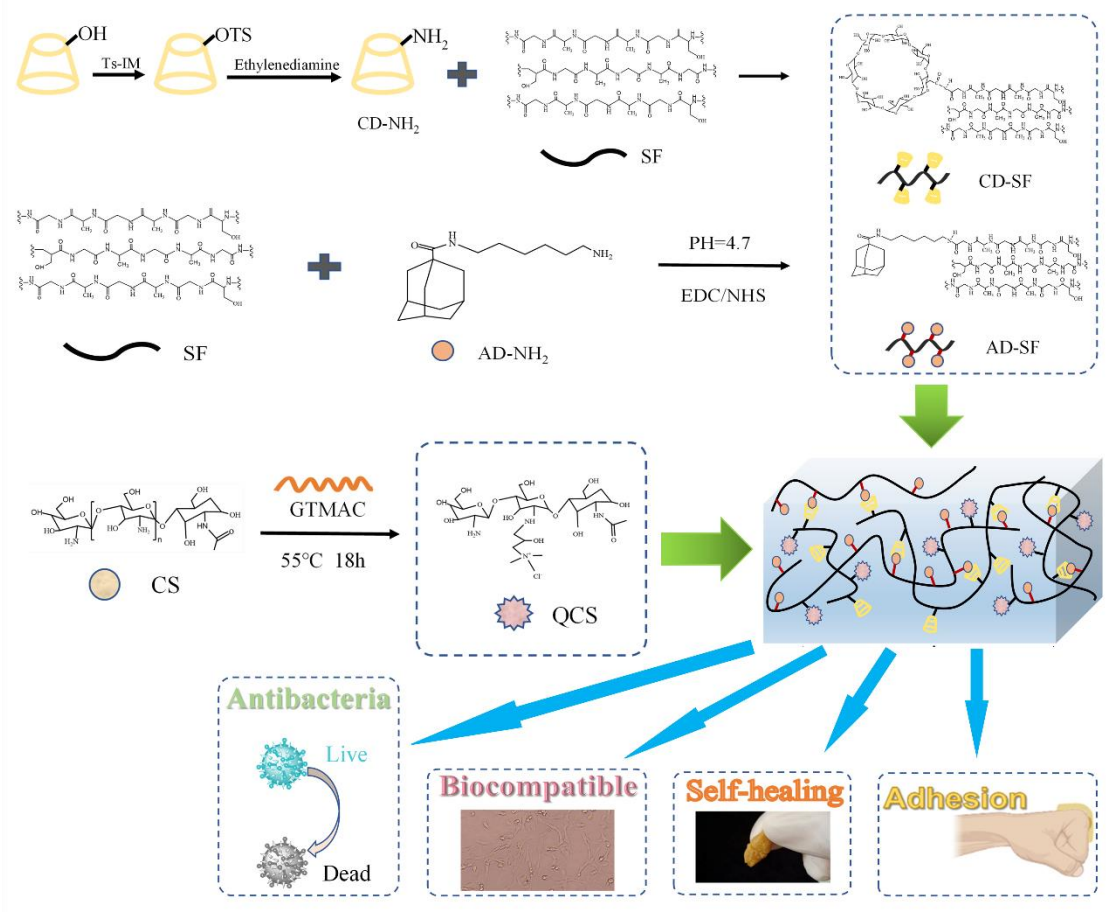

Scheme 1. Schematic diagram of fabrication of QCA hydrogels based on CD-SF, AD-SF, and QCS. Polymers CD-SF, AD-SF, and QCS were successful synthesized first, after then, QCA hydrogels were formed through the host-guest interactions between CD-SF as host polymer and AD-SF as guest polymer, with combining with QCS.

2 Materials and Methods

2.1 Materials

Silk fibroin (SF) was purchased from Shanghai Yien Chemical Technology Co.,

Ltd. Chitosan (CS) with 80-95% deacetylation degree, and 200–800 cP viscosity was purchased from Sigma-Aldrich. Dimethylimidazole ($C_4H_6N_2$ 95.0%), p-toluenesulfonyl chloride ($C_2H_7SO_2Cl$, TS-Cl 99.0%), glycidyl ammonium chloride (GTMAC), ethylenediamine (EDA), 2,2-Diphenyl-1-picrylhydrazyl (DPPH), ammonium chloride (NH_4Cl 99.5%), 1-(3-dimethylaminopropyl)-3-2-carbodiimide hydrochloride (EDC 98%), N-hydroxysuccinimide (NHS 98%), hydrochloric acid (HCl), dichloromethane (CH_2Cl_2 98%), N-hexane (C_6H_{14} 98%), sodium chloride (NaCl 99%) were purchased from Sinopharm Chemical Reagent Co., Ltd. β-Cyclodextrin ($C_{42}H_{70}O_{35}$, CD 95%) was sourced from Shanghai McLean Biochemical Technology Co., Ltd. Ethylenediamine ($C_2H_8N_2$ ≥98%) was purchased from Cayman Company. Sodium hydroxide was acquired from Xiya Reagent Co., Ltd.

2.2 Preparation of quaternary ammonium chitosan (QCS)

QCS was prepared using the modified method as previously described [20]. CS (8 g, 50 mmol) and GTMAC (3.6 g, 25 mmol) were reacted at reflux in a three-neck vessel containing 300 mL of distilled water. The reaction was mixed at 80 °C for 36 h and subsequently dialyzed for 3 days in distilled water using a dialysis membrane with a molecular weight cutoff of 14 kDa. Then, the sample was concentrated and lyophilized to obtain QCS.

2.3 Synthesis of β-cyclodextrin-modified silk fibroin (CD-SF)

CD-SF was synthesized according to the method in reference [34]. Detailed steps are as follows.

2.3.1 Preparation of 1-(p-toluensulfonyl) imidazole (TS-IM)

Dissolve 10 g of TS-Cl (52.5 mmol) in 50 mL of dry CH_2Cl_2 under nitrogen protection at 0 °C. At the same time, 8 g of dimethylimidazole (118 mmol) was dissolved in 50 mL of dried CH_2Cl_2 and then subsequently introduced to the TS-Cl solution. The mixture was stirred continuously for 8 hours at room temperature. The insoluble material was filtered out, and the mixture was concentrated using rotary evaporation at 40 °C. Then, the white crystals were precipitated with 150 mL of n-hexane and finally washed with a 1:1 mixture of n-hexane/ethyl acetate. The white precipitated crystals were dried in a vacuum to obtain TS-IM.

2.3.2 Synthesis of mono-6A-(p-toluenesulfonyl)-6A-deoxy-β-cyclodextrin (CD-OTS)

10 g of CD (8.81 mmol) and 2.5 g of TS-IM (11.23 mmol) were stirred for 4 h at 25 °C to be dissolved in 100 mL of deionized water. The mixture was then purified by adding 1 mL of NaOH solution (20 w/v%) drop by drop. Finally, the impurities were separated. The collected filtrate was neutralized with (6.91 g, 128.4 mmol) ammonium chloride to pH = 7 to get the precipitate. The white material was filtered out, washed with a mixture of acetone and cold water, and then dried in a vacuum oven (60 °C) to obtain CD-OTS.

2.3.3 Preparation of β-cyclodextrin-ethylenediamine (CD-EDA)

1 g of CD-OTS (0.77 mmol) was added to 30 mL of EDA and heated to 70 °C for complete dissolution, while stirring continuously for 14 h. After the mixture temperature was cooled to 25 °C, 40 mL of ethanol was added to the above mixture. The mixture was then filtered to produce a white solid precipitate. The precipitated CD-EDA was washed with 30 mL ethanol and, finally, vacuum dried at 55 °C for 24 h.

2.3.4 Synthesis of CD-SF

SF (0.2 g) was dissolved in 15 mL PBS buffer. Then 1-(3-dimethylaminopropyl)-3-ethylcarbodiimide (0.3 g) and n-hydroxythiosuccinimide (0.6 g) were introduced to enable complete dissolution. After 30 min, CD-EDA (1.572 g) was introduced to the solution, and the solution pH was adjusted to 4.7 using 0.01 M HCl. The reaction was carried out at room temperature for 72 h. The solution was then dialyzed in 0.1 M NaCl solution (8000 MWCO) for 2 days and then in deionized water for 1 day. Finally, the product was freeze-dried to obtain CD-SF.

2.4 Synthesis of adamantane-modified silk fibroin (AD-SF)

AD-SF was synthesized according to the method in reference [34]. 2.6 g of SF protein was dissolved in 30 mL of deionized water at 25 °C, then 3 g of EDC and 5.1 g of NHS were added and stirred for 30 min to enable complete dissolution. In the mixture, 3 g of adamantane was also further introduced and dissolved completely. The pH of the solution was adjusted with 0.01 M hydrochloric acid to pH = 4.7. The reaction was then carried out at 25 °C for 72 h. Finally, the solution was dialyzed in 0.1M NaCl solution (8000 MWCO) for 2 days followed by 1 day in deionized water. The AD-SF solution was freeze-dried to obtain the AD-SF guest polymer.

2.5 Preparation of QCA hydrogels

The synthesized polymers QCS, CD-SF and AD-SF were used to fabricate QCA hydrogels. In this paper, QCA15 and QCA20 were prepared based on the different ratios of QCS, CD-SF and AD-SF. QCS, CD-SF and AD-SF were dissolved in deionized water at 70 °C to prepare solution A, solution B, and solution C (15 w/v%),

respectively. Sample QCA15 hydrogel was prepared by mixing 20 μL of solution A (7.5 w/v%), 20 μL of solution B (15 w/v%), and 20 μL of solution C (15 w/v%) at room temperature. Sample QCA20 hydrogel was obtained by compositing 20 μL of solution A (7.5 w/v%), 20 μL of solution B (20 w/v%), and 20 μL of solution C (20 w/v%) at room temperature.

2.6 ^{1}H NMR analysis

The tested polymer was added to 1 mL of D_2O, and then the dissolved polymer was transferred to the NMR tube. The prepared samples were then subjected to H-spectral analysis using the NMR spectrometer (^{1}H NMR, 600 MHz, Proton Nuclear Magnetic Resonance Spectrometer, JEOL ECZ600R/S3).

2.7 FT-IR analysis

The Fourier Transform Infrared spectra of obtained polymers and QCA hydrogels were obtained by Attenuated Total Reflection-Fourier Transform Infrared spectroscopy (ATR-FTIR, ThermoFisher, Nicolelis5), and each spectrum was scanned 64 times on average with a resolution of 1 cm^{-1}.

2.8 SEM analysis

Field emission scanning electron microscopy (SEM, S-4800, Hitachi) was used to characterize the cross-sectional morphology of the QCS polymer. The dried samples were cut into thin slices with uniform size and thickness and then glued on a sample stage. The samples were then sprayed with platinum for 40 seconds. Finally, the hydrogel morphology was observed.

2.9 Rheological properties analysis

The DHR-2 rheometer (TA, USA) was employed to assess the rheological characteristics of the QCA hydrogels. Frequency, shear, self-healing and stress tests were conducted using aluminium low-inertia parallel plates of 40 mm diameter and with a 1 mm gap. Low-viscosity oil was placed on the outer edge of the cone during testing to prevent water evaporation [35].

2.10 Adhesive strength test

The fabricated hydrogels can be attached to different substrates and directly connected to the skin through different actions, such as arms and fingers, showing the adhesion properties of the hydrogel to various materials [36].

2.11 Self-healing properties evaluation

2.11.1 Macroscopic self-healing test

The sample was cut and divided into two segments and placed together. After a period of time, the hydrogel can be self-healed at room temperature [37].

2.11.2 Quantitative self-healing experiment

The hydrogel was placed on the parallel plates of TA rheometer. The strain amplitude scanning test was performed on the QCA hydrogel at room temperature. The amplitude oscillatory strain was transformed from a small strain of $\gamma = 1.0$ % to a large strain of $\gamma = 300$ %, with an interval of 100 s between each strain, for a total of 3 cycles to evaluate the self-healing performance of the QCA hydrogels [38].

2.12 Antioxidant activities analysis

Antioxidant activities of QCA hydrogels were investigated using DPPH radicals. QCA hydrogels were added to a mixture of ethanol and DPPH (2 mL, 0.1 mM). After

stirring and incubation for 30 min away from light, the solution was scanned with a UV-visible spectrophotometer at 200 ~ 800 nm, and the absorbance at 517 nm was measured. The DPPH scavenging rate was determined using equation (1) [12].

$$\text{DPPH scavenging (\%)} = \frac{A_0 - A_1}{A_0} * 100\% \qquad (1)$$

Where A_0 denotes the absorbance value at 517 nm for the blank group (DPPH + ethanol), and A_1 denotes the absorbance value at 517 nm for the sample group (DPPH + ethanol + sample).

2.13 In vitro biocompatibility analysis

The biocompatibility of the QCA hydrogels was evaluated by cell culture experiments to observe the cell survival rate at different incubation times. Briefly, mouse embryonic fibroblast cells (NIH-3T3) were inoculated in hydrogel extracts and incubated at 37 °C and 5 % CO_2 for 1, 3, and 5 days. Cells were cultured in a medium without adding hydrogel samples as the control group. The control and each sample were prepared in triplicate. After 1, 3, and 5 days, 10 μL of CCK-8 reagent was added, and the wavelength value at 450 nm was determined after incubation for 2 h in the incubator and transudation. NIH-3T3 were inoculated in hydrogel extracts for 24 h and 72 h, and cell morphology was observed using optical microscopy.

2.14 Antibacterial properties analysis

Solid antibacterial tests were used to evaluate the antibacterial properties of QCA hydrogels. Briefly, a bacterial suspension of 10^7 CFU mL^{-1} (100 μL) was uniformly inoculated on a nutrient AGAR (NA) plate with a diameter of 90 mm, and then the QCA hydrogel was laid flat on the nutrient AGAR plate and cultured in a humidified

incubator at 37 °C for 24 h. The antibacterial capacity of the sample was measured according to the size of the antibacterial zone.

2.15 Statistic analysis

All experiments were performed in triplicates, and results are expressed as mean ± standard deviation (SD). The SPSS software (SPSS Inc, Chicago IL) was used, and ANOVA or 2-way repeated-measures ANOVA statistical analyses were applied to investigate statistical differences, $p < 0.05$ was considered significant.

3 Results and discussion

3.1 Synthesis and characterization of QCS

First, we prepared QCS polymer, the synthetic process is shown in **Scheme 1**. QCS polymer was synthesized via grafting GMTAC on the chain of chitosan. The functional groups in QCS polymer were detected by FT-IR analysis. The characteristic peak of CS and QCS at about 1640 cm^{-1} is attributed to the carbonyl stretching vibration of the acetylated amino group [39]. The peak at 1475 cm^{-1} in the FT-IR diagram of QCS was designated as trimethylammonium group at the C-H bend (**Figure 1a**). SEM is an effective method for identifying the morphological structure and pore size of materials. The SEM images indicated that the morphology of the lyophilized QCS polymer is porous (**Figure 1b**). Furthermore, in the ^{1}H NMR spectrum of QCS, the peak value of D_2O was 4.79 ppm, and the two distinct proton characteristic peaks at 3.2 ppm and 3.5 ppm were attributed to trimethylammonium and -NH-CH_2 groups, respectively (**Figure 1c**). These results suggest that the

quaternary ammonium group was successfully grafted onto the chitosan chain.

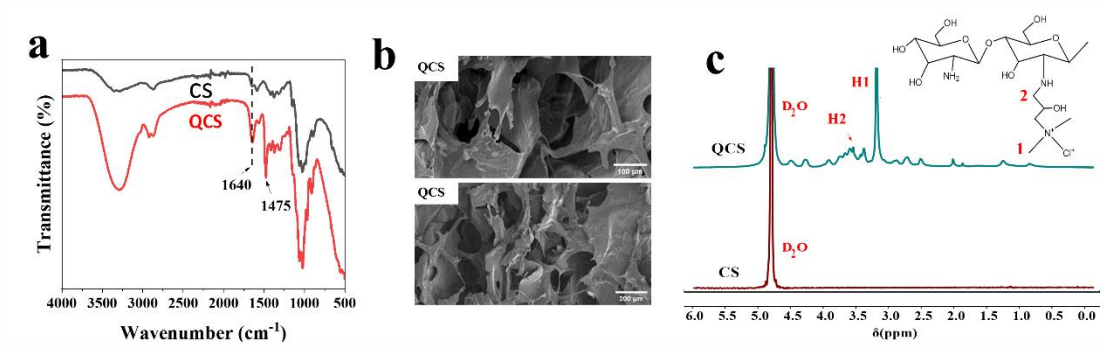

Figure 1. Synthesis and characterization of QCS polymer. (a) FT-IR spectra of polymers chitosan and QCS. (b) SEM images of QCS polymer. (c) The ^{1}H NMR spectra of chitosan and QCS (in D_2O).

3.2 Synthesis and characterization of CD-SF

β-CD is a cyclic macromolecule, essentially composed of α-D glucopyranose units joined by α-1,4 glycosidic bonds [40]. β-CD, as a host molecule, has good biocompatibility and the ability to bind to guest molecules. We prepared host polymer CD-SF (**Scheme 1**). The TS-IM was synthesized by the reaction of TS-Cl and dimethylimidazole. The CD-OTS was obtained by the reaction of TS-IM and CD, and then CD-OTS reacted with ethylenediamine to obtain CD-EDA. Finally, CD-EDA is modified onto SF backbone to obtain CD-SF polymer. ^{1}H NMR and FT-IR analysis were performed to confirm the successful synthesis of TS-IM. In ^{1}H NMR spectra (**Figure 2a)**, 2.38, 7.2-7.36, and 7.63 ppm correspond to methyl group, H4 and H5 of tosyl ring, respectively. According to FT-IR spectra, the peak of the product at 1491 cm^{-1} contributed to the stretching vibration of the methyl group of the toluene ring, and the peak at 1592 cm^{-1} is due to the stretching vibration of the imidazole group of dimethylimidazole (**Figure 2c**). These appearance peaks indicated that the TS-IM was

synthesized successfully [34, 41].

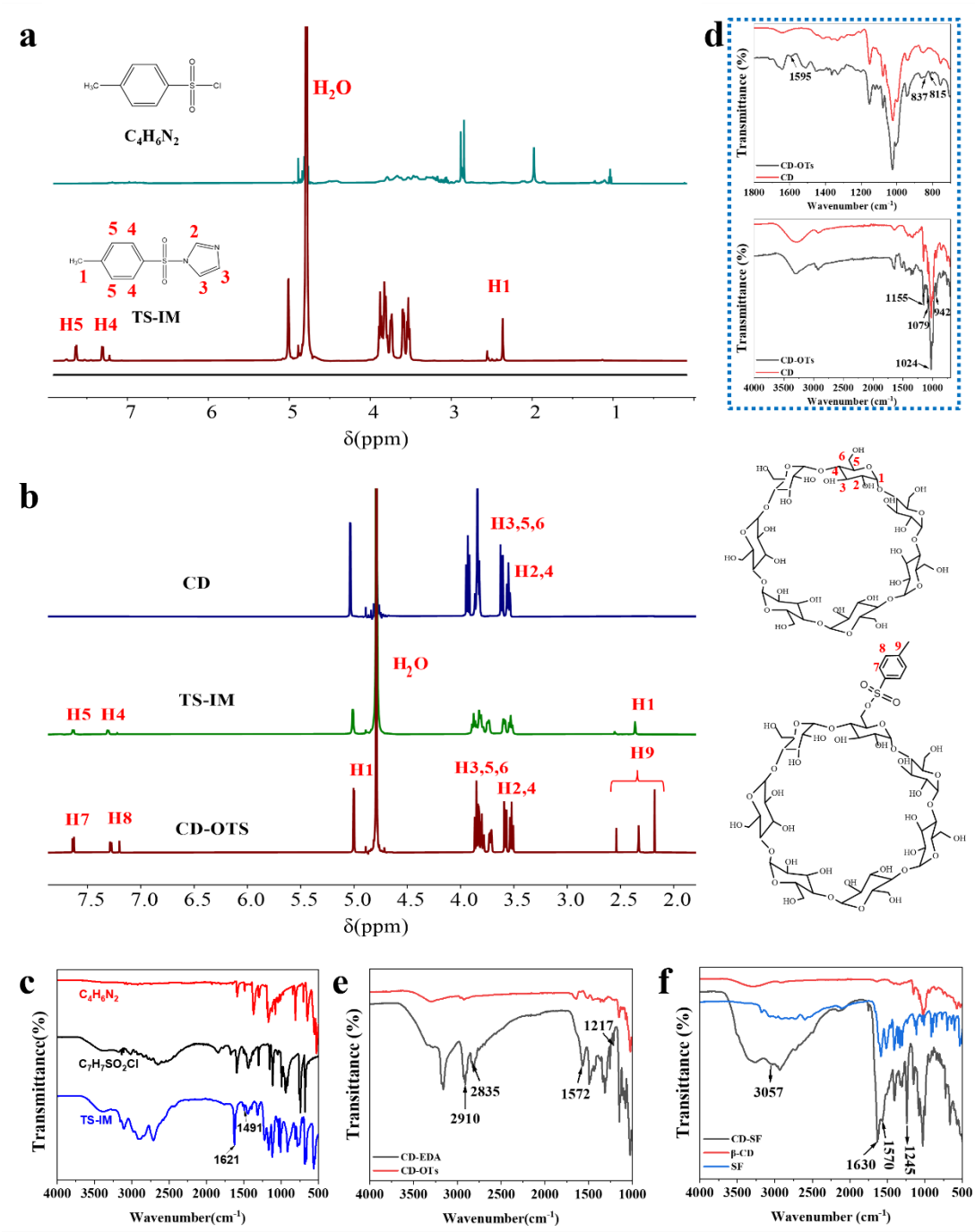

Figure 2. Synthesis and characterization of CD-SF polymers. (a) ^{1}H NMR spectra of $C_4H_6N_2$ and TS-IM. (b) ^{1}H NMR spectra of CD, TS-IM, and CD-OTS. (c) FT-IR spectra of $C_7H_7SO_2Cl$, $C_4H_6N_2$, and TS-IM. (d) FT-IR spectra of CD and CD-OTS. (e) FT-IR spectra of CD-OTS and CD-EDA. (f) FT-IR spectra of CD-SF, β-CD, and SF.

The ^{1}H NMR spectra of CD-OTS indicated that all peaks are related to CD rings after the reaction of β-CD with TS-IM, including 3.68-3.94 ppm for H3, H5 and H6, 3.43-3.61 ppm for H2 and H4, and 4.97-5.04 ppm for H1 were retained [34]. In addition, all peaks associated with the imidazole ring were maintained at 2.45, 7.44 and 7.76 ppm, which confirmed that the synthesis of CD-OTS was successful (**Figure 2b**) [34]. In the FT-IR spectra, new bands at 1595, 837 and 815 cm^{-1} are evidence for the formation of CD-OTS from cyclodextrins using benzene ring modifications (**Figure 2c** and **2d**) [42]. Furthermore, FT-IR analysis proved that CD-EDA was successfully synthesized. The peaks at 2835 cm^{-1} and 2910 cm^{-1} correspond to the stretching vibration peak of CH_2 on EDA, the absorption peak at 1572 cm^{-1} is the stretching vibration peak of N-H on the amine group of ethylenediamine, and the absorption peak at 1217 cm^{-1} corresponds to the C-N stretching vibration peak of ethylenediamine (**Figure 2e**) [34].

SF is a promising biomaterial that is highly biocompatible, non-toxic, affordable, abundant in resources, hydrophilic, and biodegradable. According to previously published research, we prepared silk fibroin from silkworm cocoon [28]. In the following step, the host polymer CD-SF was fabricated by the reaction of SF backbone and CD-EDA. The structure of the host polymer was confirmed by using FT-IR analysis. The appearance of the peak at 3057 cm^{-1} demonstrated the formation of amide bonds and the successful modification of filamentous proteins by cyclodextrins (**Figure 2f**) [34]. These results suggest that the host polymer CD-SF was successfully synthesized.

3.3 Synthesis and characterization of AD-SF

In the past few decades, AD-CD guest-host interactions have been extensively studied and are known to have a relatively high association constant of approximately 10^5 M^{-1} compared with other guest-host complexations [33]. Next, AD was selected as a guest molecule to synthesize the guest polymer AD-SF (**Scheme 1**). In FT-IR spectra of adamantane-modified SF, the appearance of a peak at 3085 cm^{-1} demonstrated the formation of amide bonds and the successful modification of filamentous proteins by adamantine (**Figure 3a**) [34]. In ^{1}H NMR spectra, the new peaks at 1.5-1.8 ppm related to adamantane groups and characteristic peaks of SF at 3.5 ppm confirmed the successful synthesis of AD-SF (**Figure 3b**) [34].

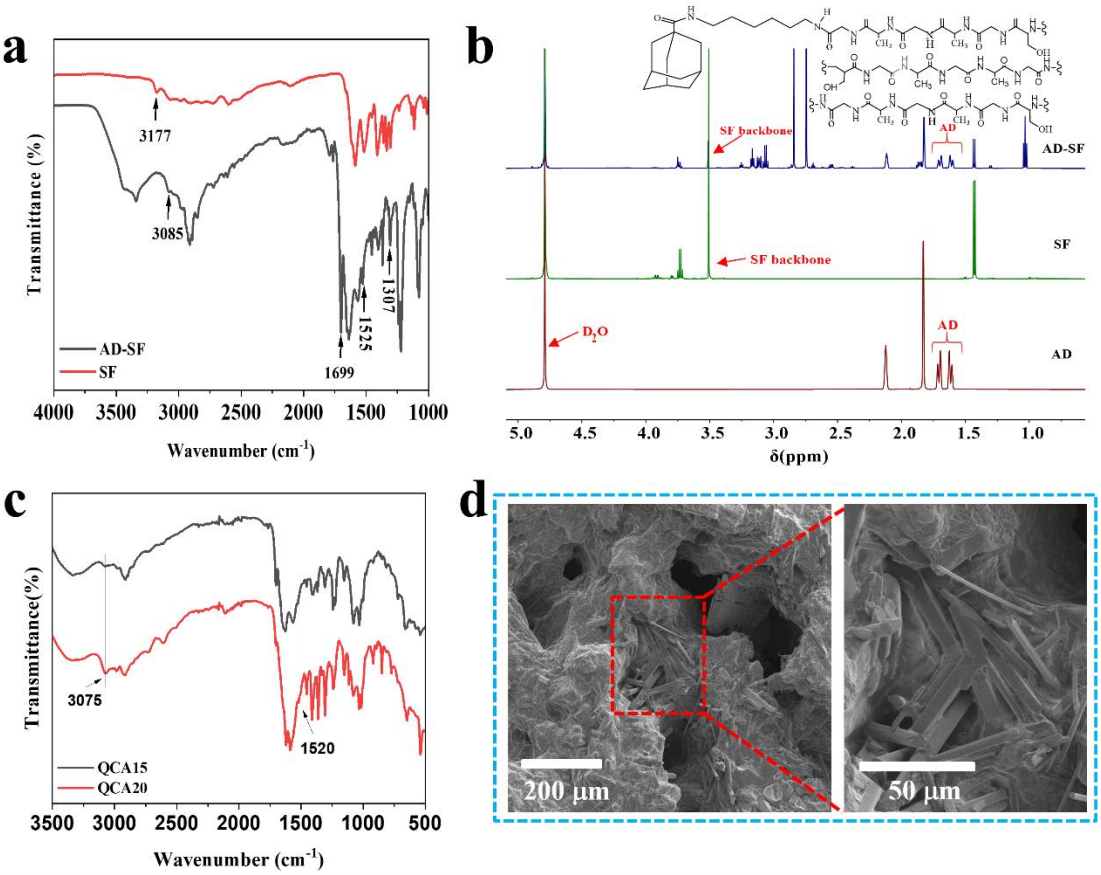

Figure 3. (a) FT-IR spectra and (b) The ^{1}H NMR spectra of SF, AD, and AD-SF, during ^{1}H NMR

test, SF, AD, and AD-SF were dissolved in D_2O. (c) FT-IR spectra and SEM image of QCA hydrogels. Note that the SEM image of QCA20 was shown due to the very similar structure between QCA15 and QCA20.

3.4 Fabrication of QCA hydrogels

AD-SF (as guest polymers), CD-SF (as host polymers), and QCS were mixed in deionized water, resulting in the rapid development of a pseudoplastic hydrogel through their reversible host-guest interaction and hydrogen-induced assembly (**Scheme 1**). In FT-IR spectra of QCA hydrogels, the appearance of a peak at 3075 cm^{-1} was attributed to the formation of amide bonds between AD-SF and CD-SF. A peak appeared at 1520 cm^{-1}, which was assigned to the methyl group (C-H) bending of QCS (**Figure 3c)** [34]. The obtained QCA hydrogels displayed an unevenly porous structure, and many fibrous structures were observed due to the presence of SF. SEM image of sample QCA20 was only shown due to the both samples had the similar microstructure (**Figure 3d**).

3.5 Rheological properties of QCA hydrogels

The rheological analysis of hydrogels is essential to understand their physical and rheological characteristics. The results are displayed in **Figure 4**. **Figure 4a** showed that both QCA15 and QCA20 hydrogels' storage modulus (G') and loss modulus (G'') continued to increase with the increase of frequency, and G' was higher than the G'', indicating that the hydrogels behaved as viscoelastic solids. As shown in **Figure 4b**, with the increase in shear rate, the viscosity of the QCA hydrogels decreased, indicating the hydrogels' shear thinning behavior. According to the strain

amplitude sweep results, within a specific range, when the strain amplitude continues to increase, G’ and G’’ appeared at an intersection point, which meet the structure failure of the QCA hydrogels. The strain value of QCA20 hydrogel network collapsed and reached 6823 %, while that of QCA15 hydrogel was only 44 %. This suggested that sample QCA20 exhibits superior strain capacity compared to sample QCA15 (**Figure 4c**). Sufficient mechanical property is essential for hydrogels to be used as biomedical-grade materials. The G′ and G″ of QCA hydrogels were recorded over time to evaluate their mechanical property. As shown in **Figure 4d**, the storage modulus value of QCA hydrogels was higher than that of the skin (G’ = 200-2000 Pa) [43]. The results suggest that QCA15 and QCA20 possess stronger mechanical properties, which could meet the basic requirements of practical application in the wound healing field.

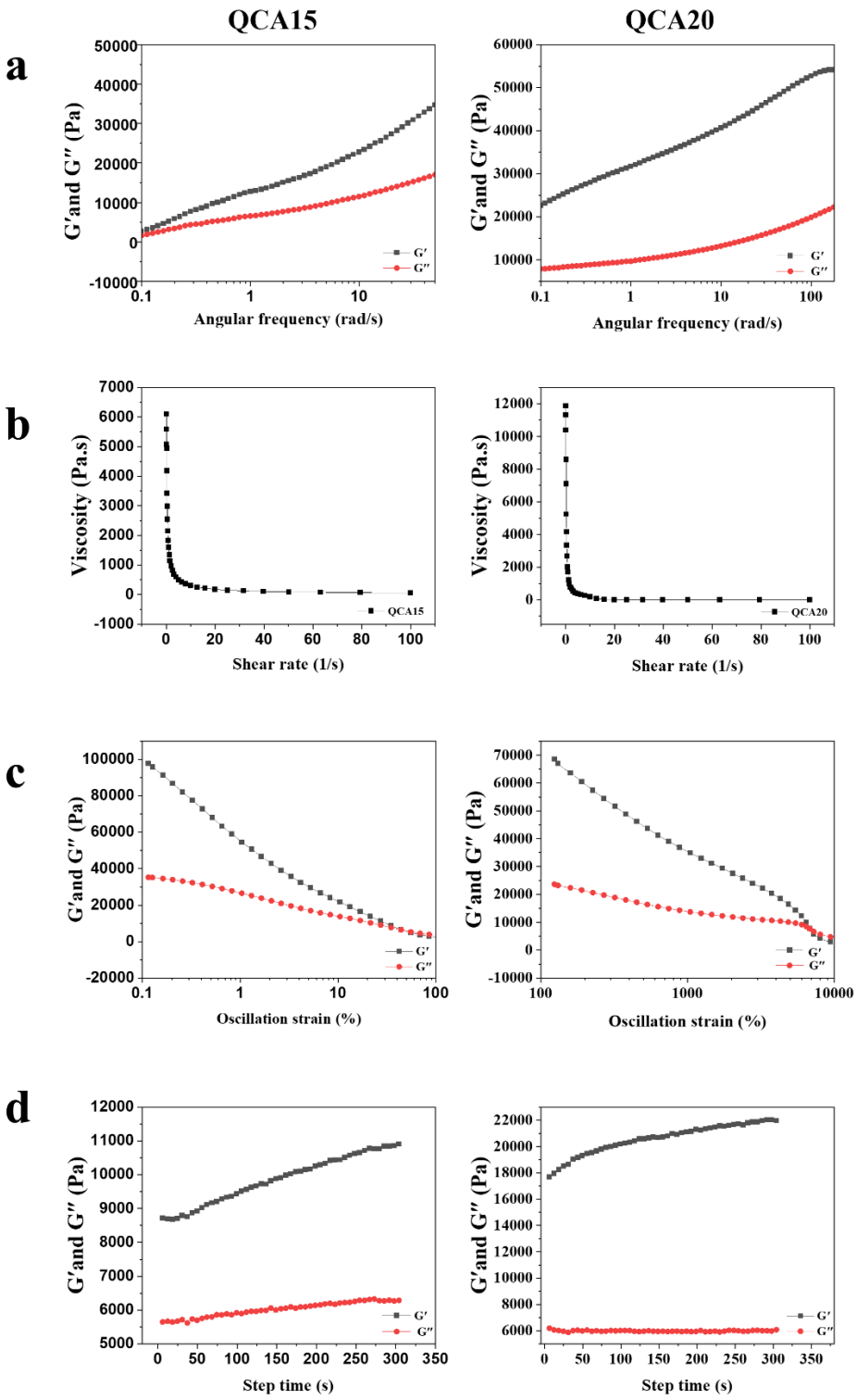

Figure 4. Rheological properties of QCA hydrogels**.** (a) The storage modulus (G') and loss modulus (G'') of QCA hydrogels were evaluated over frequency. (b) Viscosity dependence on the shear rate of QCA hydrogels. (c) G' and G'' for the strain scan of QCA hydrogels. (d) G' and G'' of hydrogels on time sweep.

3.6 Self-adhesion and self-healing performances of QCA hydrogels

In the process of wound healing, the adhesive properties of hydrogel make it close contact with the wound surface, absorb tissue exudate, block the invasion of external microorganisms, and ultimately promote wound healing [44]. Therefore, the wet adhesion abilities of the hydrogels on different substrates were investigated. QCA15 and QCA20 hydrogels could adhere to fingers, arms and glasses, which indicated that the hydrogels possess adhesive properties (**Figures 5a** and **5b**). The host-guest interaction is one of the physical crosslinking methods, which results in the shear-thinning and self-healing properties of hydrogels [32]. In order to further investigate the self-healing properties of the hydrogel, the QCA hydrogels were cut into two pieces and put together. After then, the QCA hydrogels healed without any external intervention. The self-healing process of sample QCA20 hydrogel was shown in **Figure 5c**. In **Figure 5d**, we have demonstrated that QCA hydrogels have shear-thinning properties. Subsequently, the rheological recovery behavior of QCA hydrogels was analyzed by the continuous step strain method. The cyclic test results suggested that the QCA20 hydrogel network recovered more efficiently than QCA15, which was due to the higher crosslinking density between AD-SF and CD-SF.

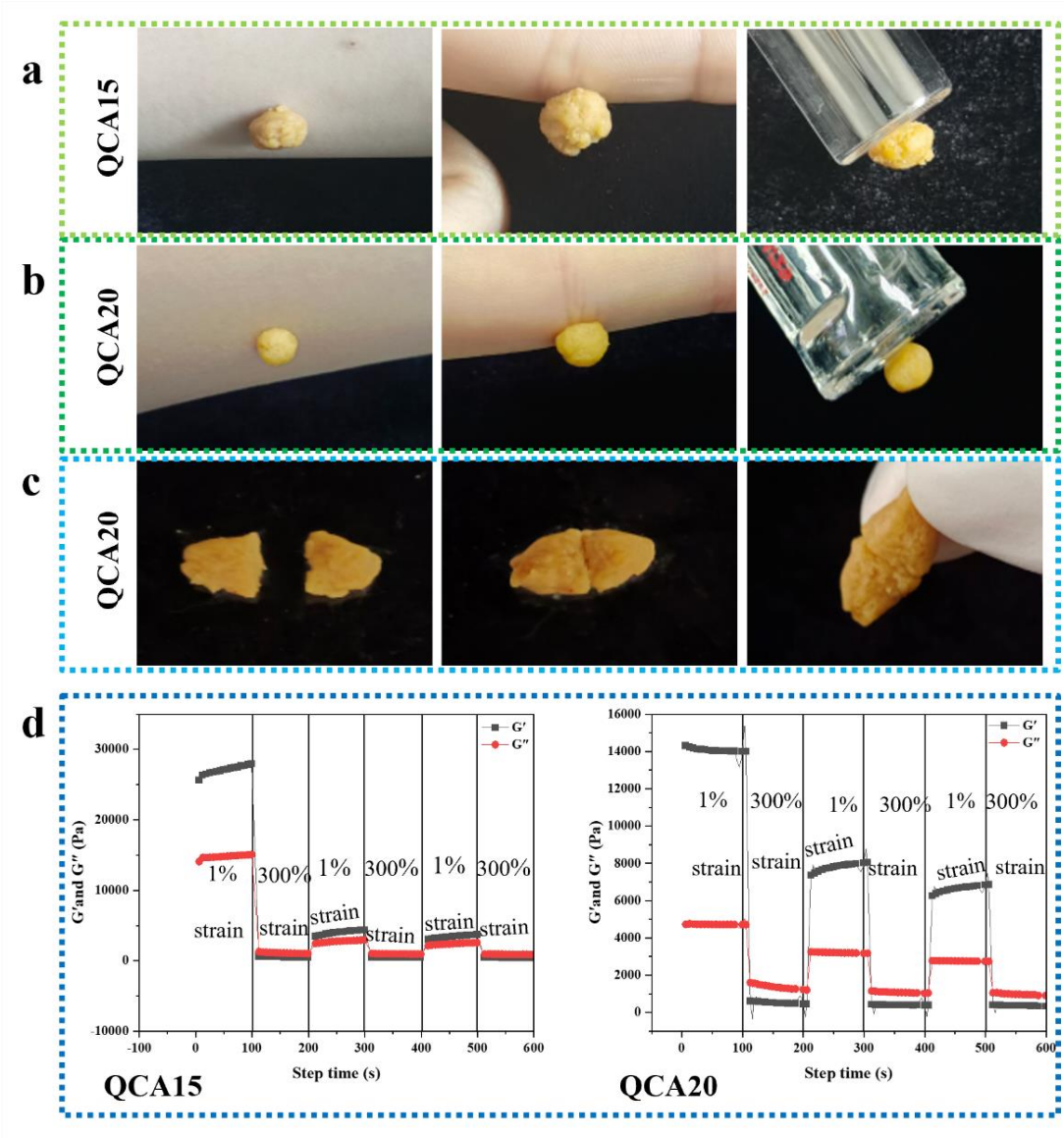

Figure 5. Self-adhesion properties of (a) QCA15 and (b) QCA20 hydrogels. (c) The self-healing process was displayed using sample QCA20 hydrogel. (d) The self-healing property of the hydrogel was tested by a rheometer (QCA hydrogels were subjected to alternate strain from 1% to 300%).

3.7 In vitro biocompatibility of QCA hydrogels

It is an essential condition for the practical application of hydrogels in biomedicine to ensure contact between materials and tissues without causing damage to tissues [45]. Biocompatibility of the QCA hydrogels was evaluated by culturing

with typical cells (NIH-3T3) via CCK-8 assays and optical microscopy investigation. In **Figure 6a**, the CCK-8 data revealed that the proliferation of NIH-3T3 cells cultured with QCA hydrogels increased over days, and cells survival rates at each time after hydrogels treatment were comparable to the group without hydrogels treatment. In addition, the increased cells growth over days could be investigated using optical microscopy images, as shown in **Figure 6b**. The optical images revealed that most of the cells treated with hydrogels had normal spindle morphology. These results indicate that the hydrogels possessed good biocompatibility. In our previous research [25, 46, 47], SF and chitosan were used to fabricate hydrogels dressings for wound healing application by compositing with other polymers or loading antibiotic drugs. In this work, the hydrogel dressings could be designed and obtained based on the host-guest interactions and hydrogen-bonding assembly from SF and chitosan.

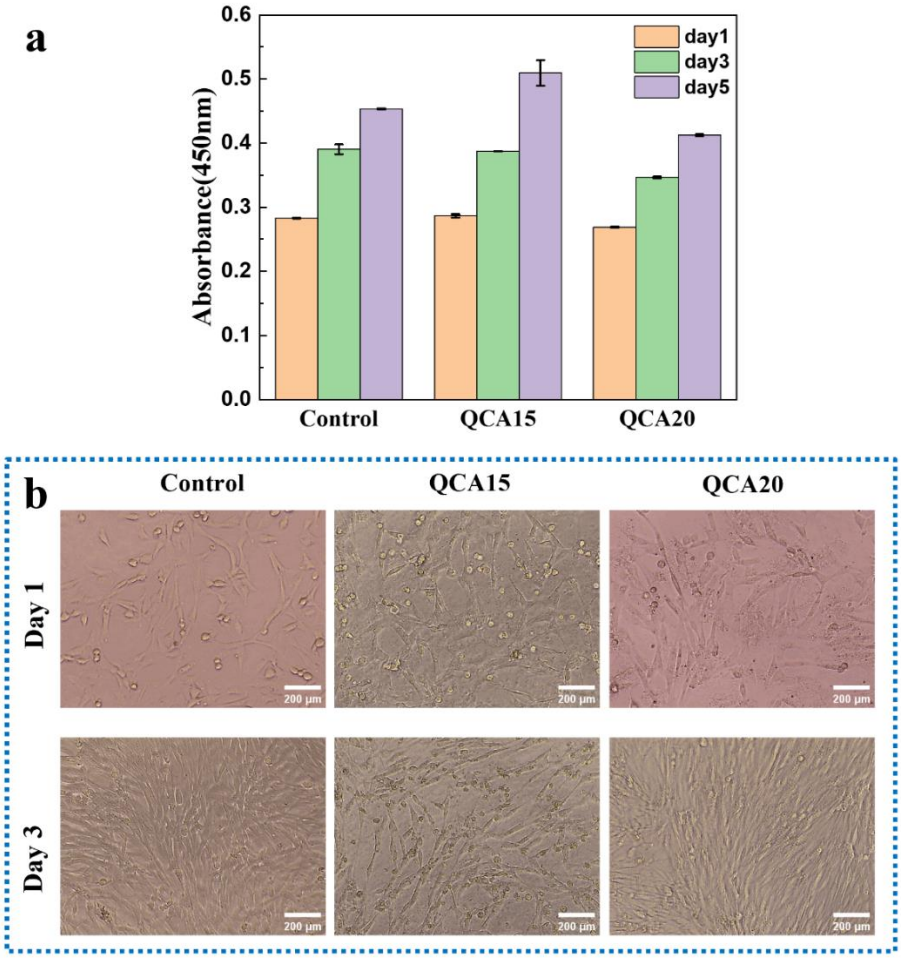

Figure 6. (a) The cytocompatibility of the QCA hydrogels was evaluated by CCK-8 assay by culturing with NIH-3T3 cells for 1, 3 and 5 days. (b) The proliferation of NIH-3T3 cells at 1 and 3 days was detected by the extraction solution method. The cell shape was recorded by optical microscope (scale: 200 μm).

3.8 Antibacterial activity and antioxidant property of QCA hydrogels

An unhealed wound that is exposed to the external environment without any protection is susceptible to infection with pathogenic microorganisms [48]. Accordingly, hydrogels have been extensively studied as an alternative material for antibacterial applications. It has been reported that chitosan-based hydrogels were used in wound treatment and had good healing effects [49-52]. Chitosan is a

positively charged cationic polymer, and most bacteria have a negative charge due to the presence of lipopolysaccharide or lipoteichoic acid on the cell wall. This suggests that the QCA hydrogels might have antibacterial properties. To investigate this hypothesis, bacteriostatic experiments against typical gram-negative bacteria (*E. coli*) and gram-positive bacteria (*S. aureus*) were performed using the method of inhibition zone. As shown in **Figures 7a** and **7b**, the bactericidal activity of the hydrogel groups with and without QCA hydrogels was performed and observed by inhibition zone parameters on the Petri dish. The hydrogels showed a broad inhibition zone, which confirmed the vital capacity of QCA hydrogels to eliminate *E. coli* and *S. aureus*. Compare to *S. aureus*, both QCA15 and QCA20 hydrogels showed better inhibition effect on *E. coli*, which was due to the different structure of bacterium cytoderm [53].

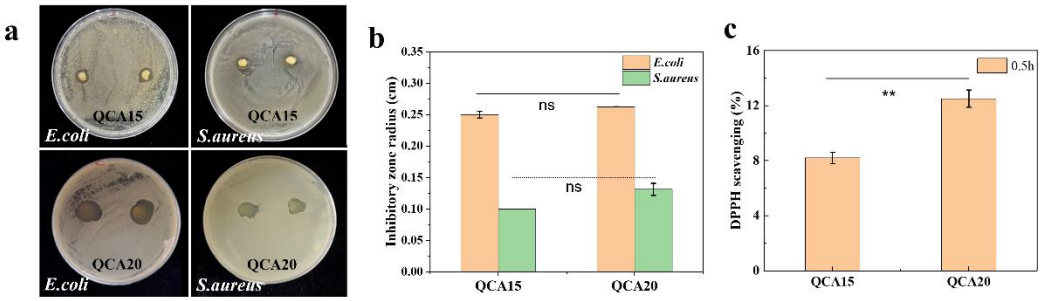

Figure 7. The antibacterial behavior of QCA hydrogels. (a) Photographs of QCA hydrogels against *E. coli* and *S. aureus*. (b) The values of inhibition zone of QCA hydrogels against *E. coli* and *S. aureus*. (c) DPPH scavenging of QCA hydrogels (0.5 h). (**$p<0.01$).

Antioxidant activity plays a positive role in inducing wound healing by regulating the overproduction of reactive oxygen species (ROS). As shown in **Figure 7c**, the QCA hydrogels presented weak antioxidant capacity, resulting in a poor DPPH scavenging effect. Chitosan's antioxidant activity primarily comes from its amino

groups, which can donate electrons and neutralize free radicals. During quarternization, many of these free amine groups are chemically modified into quaternary ammonium ions. Therefore, the availability of these amine groups for antioxidant reactions is reduced, impairing the QCA's overall antioxidant potential and quaternary ammonium groups are less efficient at donating electrons compared to free amine groups.

4 Conclusion

In the present research investigation, we designed and developed QCA hydrogel dressings. The obtained QCA hydrogels exhibited good mechanical properties and shear-thinning behavior, as confirmed by rheological tests. Antibacterial studies indicated the QCA hydrogel groups had bactericidal action against *E. coli* and *S. aureus*, which is necessary as a wound dressing. Moreover, the hydrogels exhibited self-healing properties due to the crosslinking based on host-guest interaction. In future, wound model with in vivo evaluation could be accomplished to further confirm the developed QCA hydrogels with a variety of properties as promising dressing materials to promote wound healing.

Conflicts of Competing Interest

The authors declare no competing financial interest.

Data availability

Data will be made available on request.

Acknowledgments

The authors acknowledge the help from the Analysis & Testing Center of XYNU. This research was supported by the Key Scientific Research Projects of Higher Education Institutions in Henan Province (24A430034).

Reference

[1] O. Arda, N. Goksugur, Y. Tuzun, Basic histological structure and functions of facial skin, Clin Dermatol, 32 (2014) 3-13.

[2] E.S. Chambers, M. Vukmanovic-Stejic, Skin barrier immunity and ageing, Immunology, 160 (2020) 116-125.

[3] M. Rahimnejad, S. Derakhshanfar, W. Zhong, Biomaterials and tissue engineering for scar management in wound care, Burns Trauma, 5 (2017) 4.

[4] W. Han, B. Zhou, K. Yang, X. Xiong, S. Luan, Y. Wang, Z. Xu, P. Lei, Z. Luo, J. Gao, Y. Zhan, G. Chen, L. Liang, R. Wang, S. Li, H. Xu, Biofilm-inspired adhesive and antibacterial hydrogel with tough tissue integration performance for sealing hemostasis and wound healing, Bioactive Materials, 5 (2020) 768-778.

[5] J. Wasiak, H. Cleland, F. Campbell, A. Spinks, Dressings for superficial and partial thickness burns, Cochrane Database of Systematic Reviews, (2013).

[6] A.-T. Iacob, M. Drăgan, O.-M. Ionescu, L. Profire, A. Ficai, E. Andronescu, L.G. Confederat, D. Lupașcu, An Overview of Biopolymeric Electrospun Nanofibers

Based on Polysaccharides for Wound Healing Management, Pharmaceutics, 12 (2020).

[7] I.M. El-Sherbiny, M.I. Abdel-Hamid, M. Rashad, A.S. Ali, Y.A. Azab, New calcareous soil-alginate composites for efficient uptake of Fe(III), Mn(II) and As(V) from water, Carbohydr Polym, 96 (2013) 450-459.

[8] M.J. Rowland, M. Atgie, D. Hoogland, O.A. Scherman, Preparation and Supramolecular Recognition of Multivalent Peptide-Polysaccharide Conjugates by Cucurbit[8]uril in Hydrogel Formation, Biomacromolecules, 16 (2015) 2436-2443.

[9] L. Nie, Q. Wei, J. Li, Y. Deng, X. He, X. Gao, X. Ma, S. Liu, Y. Sun, G. Jiang, Fabrication and desired properties of conductive hydrogel dressings for wound healing, RSC advances, 13 (2023) 8502-8522.

[10] L. Nie, Y. Sun, O.V. Okoro, Y. Deng, G. Jiang, A. Shavandi, Click chemistry for 3D bioprinting, Materials Horizons, (2023).

[11] Y. Zhu, Q. Zhang, X. Shi, D. Han, Hierarchical Hydrogel Composite Interfaces with Robust Mechanical Properties for Biomedical Applications, Adv Mater, 31 (2019) e1804950.

[12] S. Liu, Y. Zhao, H. Wei, L. Nie, P. Ding, H. Sun, Y. Guo, T. Chen, O.V. Okoro, A. Shavandi, Injectable hydrogels based on silk fibroin peptide grafted hydroxypropyl chitosan and oxidized microcrystalline cellulose for scarless wound healing, Colloids and Surfaces A: Physicochemical and Engineering Aspects, 647 (2022) 129062.

[13] L. Nie, J. Li, G. Lu, X. Wei, Y. Deng, S. Liu, S. Zhong, Q. Shi, R. Hou, Y. Sun, Temperature responsive hydrogel for cells encapsulation based on graphene oxide reinforced poly (N-isopropylacrylamide)/hydroxyethyl-chitosan, Materials Today

Communications, 31 (2022) 103697.

[14] B. Jia, G. Li, E. Cao, J. Luo, X. Zhao, H. Huang, Recent progress of antibacterial hydrogels in wound dressings, Mater Today Bio, 19 (2023) 100582.

[15] I. Younes, M. Rinaudo, Chitin and chitosan preparation from marine sources. Structure, properties and applications, Mar Drugs, 13 (2015) 1133-1174.

[16] S. Guo, Y. Ren, R. Chang, Y. He, D. Zhang, F. Guan, M. Yao, Injectable Self-Healing Adhesive Chitosan Hydrogel with Antioxidative, Antibacterial, and Hemostatic Activities for Rapid Hemostasis and Skin Wound Healing, ACS Appl Mater Interfaces, 14 (2022) 34455-34469.

[17] K. Huang, W. Liu, W. Wei, Y. Zhao, P. Zhuang, X. Wang, Y. Wang, Y. Hu, H. Dai, Photothermal Hydrogel Encapsulating Intelligently Bacteria-Capturing Bio-MOF for Infectious Wound Healing, ACS Nano, 16 (2022) 19491-19508.

[18] Z.-x. Cai, X.-m. Mo, K.-h. Zhang, L.-p. Fan, A.-l. Yin, C.-l. He, H.-s. Wang, Fabrication of Chitosan/Silk Fibroin Composite Nanofibers for Wound-dressing Applications, International Journal of Molecular Sciences, 11 (2010) 3529-3539.

[19] S. Guang, Y. An, F. Ke, D. Zhao, Y. Shen, H. Xu, Chitosan/silk fibroin composite scaffolds for wound dressing, Journal of Applied Polymer Science, 132 (2015) n/a-n/a.

[20] L. Nie, Q. Wei, M. Sun, P. Ding, L. Wang, Y. Sun, X. Ding, O.V. Okoro, G. Jiang, A. Shavandi, Injectable, self-healing, transparent, and antibacterial hydrogels based on chitosan and dextran for wound dressings, International journal of biological macromolecules, 233 (2023) 123494.

[21] L. Nie, D. Chen, S. Zhong, Q. Shi, Y. Sun, C. Politis, A. Shavandi, Injectable

cell-laden poly (N-isopropylacrylamide)/chitosan hydrogel reinforced via graphene oxide and incorporated with dual-growth factors, Materials Letters, 280 (2020) 128572.

[22] Z. Zhou, J. Cui, S. Wu, Z. Geng, J. Su, Silk fibroin-based biomaterials for cartilage/osteochondral repair, Theranostics, 12 (2022) 5103-5124.

[23] L. Mazurek, M. Szudzik, M. Rybka, M. Konop, Silk Fibroin Biomaterials and Their Beneficial Role in Skin Wound Healing, Biomolecules, 12 (2022).

[24] M.T. Sultan, O.J. Lee, S.H. Kim, H.W. Ju, C.H. Park, Silk Fibroin in Wound Healing Process, Adv Exp Med Biol, 1077 (2018) 115-126.

[25] Y. Jing, L. Ruan, G. Jiang, L. Nie, A. Shavandi, Y. Sun, J. Xu, X. Shao, J. Zhu, Regenerated silk fibroin and alginate composite hydrogel dressings loaded with curcumin nanoparticles for bacterial-infected wound closure, Biomaterials Advances, 149 (2023) 213405.

[26] B. Kundu, R. Rajkhowa, S.C. Kundu, X. Wang, Silk fibroin biomaterials for tissue regenerations, Adv Drug Deliv Rev, 65 (2013) 457-470.

[27] X. Zhang, M.R. Reagan, D.L. Kaplan, Electrospun silk biomaterial scaffolds for regenerative medicine, Adv Drug Deliv Rev, 61 (2009) 988-1006.

[28] D. Chen, P. Chang, P. Ding, S. Liu, Q. Rao, O.V. Okoro, L. Wang, L. Fan, A. Shavandi, L. Nie, MSCs-laden silk Fibroin/GelMA hydrogels with incorporation of platelet-rich plasma for chondrogenic construct, Heliyon, 9 (2023).

[29] Z. Gu, H. Xie, C. Huang, L. Li, X. Yu, Preparation of chitosan/silk fibroin blending membrane fixed with alginate dialdehyde for wound dressing, International

Journal of Biological Macromolecules, 58 (2013) 121-126.

[30] D.L. Taylor, M. In Het Panhuis, Self-Healing Hydrogels, Adv Mater, 28 (2016) 9060-9093.

[31] G. Narayanan, J. Shen, R. Boy, B.S. Gupta, A.E. Tonelli, Aliphatic Polyester Nanofibers Functionalized with Cyclodextrins and Cyclodextrin-Guest Inclusion Complexes, Polymers (Basel), 10 (2018).

[32] V.G. Muir, J.A. Burdick, Chemically Modified Biopolymers for the Formation of Biomedical Hydrogels, Chemical Reviews, 121 (2020) 10908-10949.

[33] G. Chen, M. Jiang, Cyclodextrin-based inclusion complexation bridging supramolecular chemistry and macromolecular self-assembly, Chem Soc Rev, 40 (2011) 2254-2266.

[34] M. Mohamadhoseini, Z. Mohamadnia, Alginate-based self-healing hydrogels assembled by dual cross-linking strategy: Fabrication and evaluation of mechanical properties, International Journal of Biological Macromolecules, 191 (2021) 139-151.

[35] Q. Wu, L. Wang, P. Ding, Y. Deng, O.V. Okoro, A. Shavandi, L. Nie, Mercaptolated chitosan/methacrylate gelatin composite hydrogel for potential wound healing applications, Composites Communications, 35 (2022) 101344.

[36] R. Dang, L. Chen, F. Sefat, X. Li, S. Liu, X. Yuan, X. Ning, Y.S. Zhang, P. Ji, X. Zhang, A Natural Hydrogel with Prohealing Properties Enhances Tendon Regeneration, Small, 18 (2022) e2105255.

[37] X. Jing, H. Li, H.-Y. Mi, Y.-J. Liu, P.-Y. Feng, Y.-M. Tan, L.-S. Turng, Highly transparent, stretchable, and rapid self-healing polyvinyl alcohol/cellulose nanofibril

hydrogel sensors for sensitive pressure sensing and human motion detection, Sensors and Actuators B: Chemical, 295 (2019) 159-167.

[38] X. Zhao, H. Wu, B. Guo, R. Dong, Y. Qiu, P.X. Ma, Antibacterial anti-oxidant electroactive injectable hydrogel as self-healing wound dressing with hemostasis and adhesiveness for cutaneous wound healing, Biomaterials, 122 (2017) 34-47.

[39] J. He, Y. Liang, M. Shi, B. Guo, Anti-oxidant electroactive and antibacterial nanofibrous wound dressings based on poly(ε-caprolactone)/quaternized chitosan-graft-polyaniline for full-thickness skin wound healing, Chemical Engineering Journal, 385 (2020).

[40] N. Tarannum, Suhani, D. Kumar, Synthesis, characterization and applications of copolymer of β–cyclodextrin: A review, Journal of Polymer Research, 27 (2020) 1-30.

[41] W. Tang, S.C. Ng, Synthesis of cationic single-isomer cyclodextrins for the chiral separation of amino acids and anionic pharmaceuticals, Nat Protoc, 2 (2007) 3195-3200.

[42] Y. Gao, G. Li, Z. Zhou, L. Guo, X. Liu, Supramolecular assembly of poly(beta-cyclodextrin) block copolymer and benzimidazole-poly(epsilon-caprolactone) based on host-guest recognition for drug delivery, Colloids Surf B Biointerfaces, 160 (2017) 364-371.

[43] Y. Yin, Q. Xu, X. Wei, Q. Ma, D. Li, J. Zhao, Rosmarinic Acid-Grafted Dextran/Gelatin Hydrogel as a Wound Dressing with Improved Properties: Strong Tissue Adhesion, Antibacterial, Antioxidant and Anti-Inflammatory, Molecules, 28 (2023).

[44] H. Jafari, P. Ghaffari-Bohlouli, M. Alishahi, F. Davani, S.S. Daneshi, R. Heidari, M.H. Morowvat, S.V. Niknezhad, L. Nie, H. Savoji, Tissue adhesive hydrogel based on upcycled proteins and plant polyphenols for enhanced wound healing, Materials Today Chemistry, 33 (2023) 101722.

[45] Y. Yuan, S. Shen, D. Fan, A physicochemical double cross-linked multifunctional hydrogel for dynamic burn wound healing: shape adaptability, injectable self-healing property and enhanced adhesion, Biomaterials, 276 (2021) 120838.

[46] L. Nie, Q. Wei, J. Li, C. Zhao, P. Ding, O.V. Okoro, A. Shavandi, Chitosan Nanocomposites: Chitosan-Based Nanocomposites as Efficient Wound Dressing Materials, Chitosan-Based Nanocomposites as Efficient Wound Dressing Materials, (2023).

[47] P. Ding, Q. Wei, N. Tian, X. Ding, L. Wang, B. Wang, O.V. Okoro, A. Shavandi, L. Nie, Enzymatically crosslinked hydrogel based on tyramine modified gelatin and sialylated chitosan, Biomedical Materials, 18 (2022) 015006.

[48] Y. Wang, Y. Wu, L. Long, L. Yang, D. Fu, C. Hu, Q. Kong, Y. Wang, Inflammation-Responsive Drug-Loaded Hydrogels with Sequential Hemostasis, Antibacterial, and Anti-Inflammatory Behavior for Chronically Infected Diabetic Wound Treatment, ACS Appl Mater Interfaces, 13 (2021) 33584-33599.

[49] T. Yan, S. Kong, Q. Ouyang, C. Li, T. Hou, Y. Chen, S. Li, Chitosan-Gentamicin Conjugate Hydrogel Promoting Skin Scald Repair, Mar Drugs, 18 (2020).

[50] X. Zhang, G.H. Sun, M.P. Tian, Y.N. Wang, C.C. Qu, X.J. Cheng, C. Feng, X.G. Chen, Mussel-inspired antibacterial polydopamine/chitosan/temperature-responsive

hydrogels for rapid hemostasis, Int J Biol Macromol, 138 (2019) 321-333.

[51] A. Rasool, S. Ata, A. Islam, Stimuli responsive biopolymer (chitosan) based blend hydrogels for wound healing application, Carbohydr Polym, 203 (2019) 423-429.

[52] H. Jafari, P. Ghaffari-Bohlouli, D. Podstawczyk, L. Nie, A. Shavandi, Tannic acid post-treatment of enzymatically crosslinked chitosan-alginate hydrogels for biomedical applications, Carbohydrate polymers, 295 (2022) 119844.

[53] T. Zhou, J. Liu, X. Zhang, B. Shen, J. Yang, W. Hu, L. Liu, The antibacterial W-containing microarc oxidation coating on Ti6Al4V, Surface and Coatings Technology, 374 (2019) 242-252.